

DIRECT FREEFORM FABRICATION OF SPATIALLY HETEROGENEOUS LIVING PRE-CELL-SEEDED IMPLANTS

D. Cohen, E. Malone, H. Lipson, and L. Bonassar

Department of Mechanical and Aerospace Engineering, Cornell University, Ithaca, NY 14850

ABSTRACT

The objectives of this work are the development of the processes, materials, and tooling to directly “3-D print” living, pre-seeded, patient-specific implants of spatially heterogeneous compositions. The research presented herein attempts to overcome some of the challenges to scaffolding, such as the difficulty of producing spatially heterogeneous implants that require varied seeding densities and/or cell-type distributions. In the proposed approach, living implants are fabricated by the layer-wise deposition of pre-cell-seeded alginate hydrogel. Although alginate hydrogels have been previously used to mold living implants, the properties of the alginate formulations used for molding were not suitable for 3-D printing. In addition to changing the formulation to make the alginate hydrogels “printable,” we developed a robotic hydrogel deposition system and supporting CAD software to deposit the gel in arbitrary geometries. We demonstrated this technology’s capabilities by printing alginate gel implants of multiple materials with various spatial heterogeneities, including, implants with completely embedded material clusters. The process was determined to be both viable ($94\pm 5\%$ $n=15$) and sterile (less than one bacterium per $0.9\ \mu\text{L}$ after 8 days of incubation). Additionally, we demonstrated the printing of a meniscus cartilage-shaped gel generated directly from a CT Scan. The proposed approach may hold advantages over other tissue printing efforts [4,5]. This technology has the potential to overcome challenges to scaffolding and could enable the efficient fabrication of spatially heterogeneous, patient-specific, living implants.

INTRODUCTION

Alginate gels have been previously used for molding of living implants. One of the aims of this research was to change the formulation in order to make it suitable for printing. Alginate is a seaweed derivate which, when combined with certain calcium cross-linking compounds, forms a polymer hydrogel [1]. Cells can be evenly mixed into this gel and then injection molded in order to create a desired geometry [2]. When the cell-seeded gel is placed in a growth medium and incubated, the cells consume the medium and replace the alginate gel, resulting in living tissue. The material properties of the gel are governed by the type of alginate, the type of cross-linker, the concentrations of each, as well as other factors such as temperature and age. The material properties that are optimal for molding the gels are not the same as those required for printing the gels. In fact, it turns out that the desired material properties for both cases are essentially opposite of each other. The discrepancies between the material properties required for molding and printing pose a major design challenge that this project addresses. The type of cell that is seeded into the gel can also dictate the required material properties. In this research, bovine cartilage chondrocyte cells are used because they do not require a blood supply for nutrition, but the challenge of growing cells that do require a blood supply is a separate open research field. Another consideration when dealing with alginate gels is the need for sterility.

Much in the same way that the alginate gel supports growth of seeded cells, it will also support the growth of bacteria and fungi; hence, sterile print conditions are essential to prevent infection.

GEL PRINTING SYSTEM

Robotic Test Platform

The Cornell Computational Synthesis Laboratory (CCSL) designed an open-architecture gantry robot that was used in this research. The tool paths are generated by custom CCSL software that takes stereo lithography (STL) files as input. This system has been designed to allow the printing of multiple materials within a single part; in this research, this capability is used to print multiple gels with varying cell types, chemical concentrations, cell densities, etc. The robot is capable of moving the deposition tool to a specified position with accuracy of $\pm 25 \mu\text{m}$ and precision of $\pm 25 \mu\text{m}$. Full robotic system specifications are given in Table 1.

Table 1 - Fabrication System Performance Specifications

Minimum material stream/drop diameter	250 μm	0.010 in.
Materials cross-section area	4.9 X 10 ⁻⁸ m ²	
Build rate	2.5 X 10 ⁻⁹ m ³ /s	0.55 in. ³ /h
Nominal speed along path	0.05 m/s	
Min. turn radius at nominal speed	125 μm	4.92 X 10 ⁻³ in
Tool position accuracy (\pm)	25 μm	9.84 X 10 ⁻⁴ in
Tool position repeatability (\pm)	25 μm	9.84 X 10 ⁻⁴ in
Positioning resolution	5 μm	1.97 X 10 ⁻⁴ in.
Build envelope x	0.3 m	11.8 in.
Build envelope y	0.3 m	11.8 in.
Build envelope z	0.3 m	11.8 in.
Max. XY acceleration	20.75 m/s ²	2.12 g

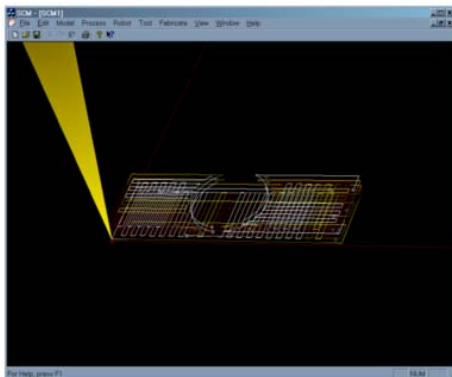


Figure 1 - Screenshot of Slicing Software As It Prepares a CAD Model for Layer-wise Fabrication

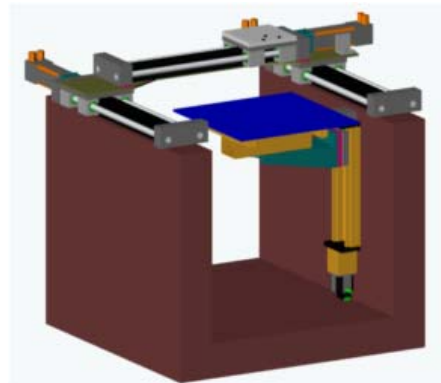


Figure 2 - CAD Model of the Gantry Robotic Test Platform

Gel Deposition Tool

The gel deposition tool needs to accurately deposit gels while maintaining sterility. Additionally, the tool has to enable efficient material changing. Efficient swapping of sterile materials is important for printing implants of multiple gels (each with different cell types, concentrations, etc.).

Through experimentation, we found that elastic materials are difficult to deposit with pneumatic dispensing systems and instead a volumetrically controlled dispensing system was chosen [3]. An ABS plastic rapid prototyped frame connects a linear actuator to the syringe cartridge (Fig. 3). Medical-quality sterile syringes are used as the disposable material cartridges of the deposition tool. Luer lock syringes were selected in order to enable a wide variety of syringe tips to be utilized. Tool performance specification can be found in table 2.

Table 2 – Deposition Tool Performance Specifications

Maximum applied pressure	1592 kPa
Cartridge volume	10 mL
Maximum volumetric flow rate	10.6 mL/s
Deposition accuracy	0.000426 mL
Deposition precision	0.000426 mL

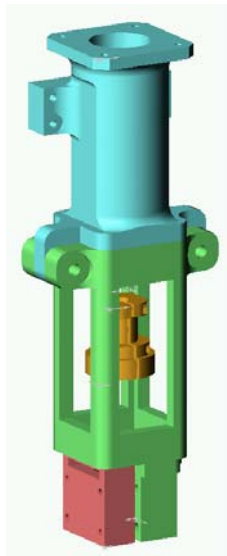


Figure 3 - CAD Model of Rapid Prototyped Deposition Tool Components (Linear Actuator and Syringe Not Shown)

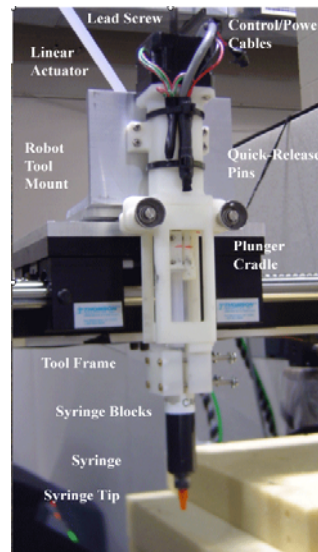


Figure 4 - Picture of Deposition Tool with Disposable Syringe Attached (Mounted To Robot's Tool Platform)

Sterile Printing Envelope

Sterile printing conditions are a paramount concern, the lack of which would allow the printed implants to become infected. Although, as described above, a solution was found for keeping the material sterile during deposition, a way of keeping the printed pieces' immediate environment sterile still needed to be found.

One possible solution to this challenge was to build a sterile, hermetically sealed envelope around the immediate printing zone. While a full envelope that encompassed the printer was considered, an even smaller envelope that surrounds only the printed piece was more desirable.

A 1-millimeter thick, autoclavable, clear plastic bag was chosen as the envelope. This bag could be loaded with a Pyrex Petri dish, sealed, and then autoclaved to ensure that the entire inside of the bag, including the Petri dish, was sterile. At this point, the inside of the bag served as a closed, sterile environment (Fig. 5). At the time of printing, the tip of the syringe and a section of the outside surface of the bag were swabbed with 70% ethanol solution and then the syringe tip was inserted through the bag. All deposited material was printed onto the sterilized Petri dish and surrounded by the previously autoclaved environment. After printing, the bag was taken to a sterile work hood where the outside of the bag was sprayed with alcohol and the sample was removed (Fig. 6). The disposable autoclave bag could then be discarded and a new bag used for the next print.



Figure 5 – Top View of Sterile Printing Envelope

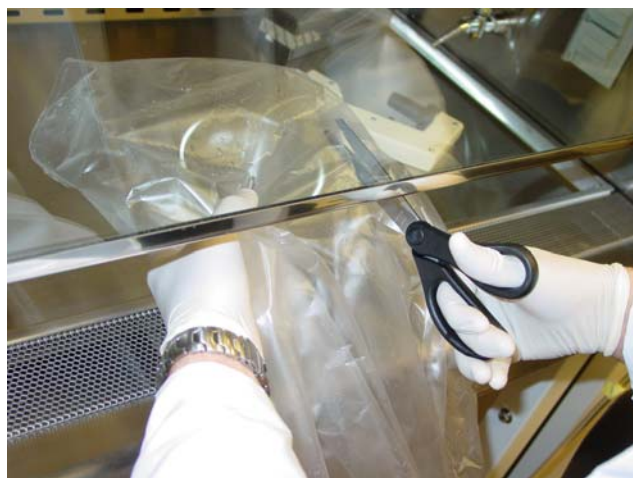


Figure 6 - Sterile Sample Being Removed From Envelope Under Ultra Violet (UV) Sterilized Hood

PRINTABLE GEL FORMULATION

The gel is composed of two components: a solution of alginate and a calcium cross-linker solution. Even though there are only two components, there were many experimental

variables and it was a challenge to find a gel that was both supportive of cellular life and “printable.”

Formulation Constraints

The alginate gel had to be both suitable from biological and SFF standpoints. In order for a gel to be considered biologically suitable, the alginate gel had to sustain cellular life.

In order to satisfy the SFF needs, the gel had to be “printable.” By “printable,” it is meant that the gel would: 1) bond between layers, 2) hold its shape against gravity, and 3) cross-link slowly enough to prevent cell and material shearing during printing.

Formulation Process

The first step was the identification of experimental parameters. These parameters were identified as: 1) the type of cross-linker, 2) the cross-linker concentration, 3) the molecular weight of the alginate 4) the M/G ratio¹ of the alginate, 5) the concentration of the alginate, 6), how long to mix the alginate and cross-linker together and with what force 7), how long to let the gel cross-link before printing, 8) the choice of additives, and 9) the range of syringe tip diameters that can be used to print the gel.

Since two separate sets of needs, biological and SFF, had to be satisfied by some single combination of the above nine parameters, each parameter’s effect on the biological and SFF qualities of the materials had to be analyzed.

Biological Formulation Needs

From prior publications [6], it was clear that the gel would most likely be viable, i.e., support cellular life, as long as the alginate concentration was 2% in PBS² and the cross-linker concentration was less than or equal to 2% in PBS. A standard seeding density of 50 million cells per milliliter of gel was also used. These established standards gave reason to believe that as long as the standards were adhered to, the biological needs would be satisfied. Also, the standards served to constrain two parameters, hence they simplified the formulation process by eliminating two variables.

SFF Formulation Needs

While the biological needs were satisfied by the aforementioned published standards, the SFF-related needs had yet to be satisfied. Extensive experimentation ensued in order to determine what effects the nine parameters had on the three SFF-related material properties: 1) bonding between layers, 2) resistance to weight induced deformation, and 3) prevention of shearing due to rapid cross-linking.

¹ M/G ratio is the mannuronic acid to guluronic acid ratio

² PBS (Phosphate-Buffered Saline) is an isotonic solution that is commonly used as a dilution agent when making hydrogels

Inter-layer Bonding Experiments

To study the effects of the nine parameters on the first SFF-related need, bonding between layers, it was determined that this behavior was directly related to the rate and amount of cross-linking at the time of printing. Gels that cross-linked more quickly would be further cross-linked at the time of deposition and would be less receptive to subsequent layers because the bonds were already formed before the following layers could be deposited. Experiments were run in which the experimental parameters were varied and the cross-linking rate was given a relative, qualitative measure depending on how quickly the gel stiffened. The relationships between the experimental parameters and the ability of the gel to bond between layers are summarized in Table 3. The goal of this experiment was to find some combination of the nine parameters that yielded a gel which cross-linked as quickly as possible, yet still bonded between layers.

Table 3 - Relationship Between Parameters and Successful Interlayer Bonding

Experimental Parameter	Relationship with Successful Bonding Between Layers
Increased alginate molecular weight	(-)
Increased cross-linker concentration	(-)
Longer mixing time	(-)
Longer sitting time before printing	(-)
Larger tip diameter	(+)

Resistance to Weight-Induced Deformation Experiments

In order to see what effect each parameter had on the second SFF-related need, resistance to weight deformation, each parameter's effect on the gel viscosity was studied using an automatic viscometer. It was initially thought that the viscosity would be an accurate indication of how well the gel would hold its shape against gravity. In order to further vary the viscosity, dextrose was used as a bulking agent. However, after comparing the results of the viscosity experiments to simulated prints in which the gel was layered by hand, it was clear that viscosity was not an accurate indicator of a gel's resistance to weight-induced deformation. The notion was rejected and this part of the formulation process was iterated. At this point, it was noticed that the resistance was strongly related to cross-linking rate. While a high viscosity did not help the gel hold its shape, partial cross-linking did; therefore, the faster a gel cross-linked the better it would be able to hold its own weight. At this point, it was realized that two SFF-related needs were directly determined by cross-linking rate, that is, the bonding between layers and the resistance to gravity. However, these two needs were opposed to each other. A higher cross-linking rate would help the gel hold its shape against gravity, while at the same time it would make the layers less likely to bond with each other. Some acceptable compromise needed to be reached.

Table 4 - Relationship Between Parameters and Resistance to Weight-Induced Deformation

Experimental Parameter	Relationship with Resistance to Weight-Induced Deformation
Increased alginate molecular weight	(+)
Increased cross-linker concentration	(+)
Longer mixing time	(+)
Longer sitting time before printing	(+)
Larger tip diameter	(+)

Cross-linking Rate Experiments

The third SFF-related need was also directly related to cross-linking rate; this was prevention of material shearing due to rapid cross-linking. If the material cross-linked too quickly, then the gel would significantly bond before being deposited and the bonds would be sheared upon passing through the constricted syringe tip. A summary of the relationship between cross-linking rates and the SFF-related needs can be found in Table 5.

Table 5 - Effect of Cross-linking Rate on SFF Needs

SFF-Related Need	High Cross-linking Rate	Low Cross-linking Rate
Bonding Between Layers	Layers will not bond with each other (-)	Layers will bond with each other (+)
Resistance to Gravity	Gel can hold shape (+)	Gel cannot hold shape (-)
Prevention of Shearing	Gel will shear and lose mechanical properties (-)	Gel will not shear (+)

Manual Test Prints

In order to find a cross-linker type/concentration that was suitable for the three SFF formulation constraints, various chemical combinations were tested manually (fig. 7). An efficient and simple test that indicates a particular formulation's printability is a conical stacking experiment. One half inch to one inch cones are deposited manually over a time range from $t = 0$ to $t = 20$ minutes. Each stacks ability to hold its shape against gravity is observed. Since the material properties are time dependent, testing over a large time period is important. Not only are qualitative traits noted for each formulation, but also an optimal time frame for each formulation is identified. In this optimal time frame, the properties are suitable for printing. With some formulations the optimal frame begins at $t = 0$, but with others the optimal time window begins after a delay. The goal was to find a printable formulation with longest optimal time window.

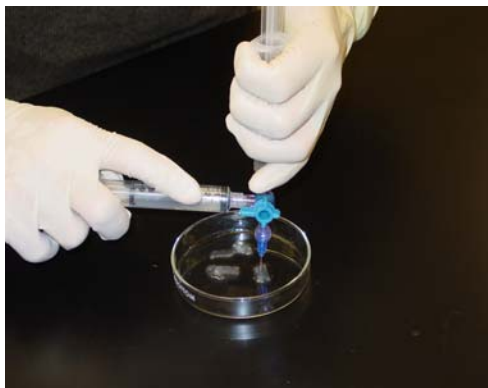


Figure 7 – Manual Print Simulation for Testing Material Properties

Selected Formulation

Although we regularly use gel formulations of various cross-linkers, alginate-types, and mixing styles, the formulation used in the experiments reported herein is 2% Protanal Alginate (a high M-group alginate) in PBS and 0.5% Calcium Sulfate in PBS. The two solutions were mixed with each other in a 2:1 alginate to CaSO_4 ratio. Since the mixing technique greatly affects the resulting gel, due to shear effects, it is important to mix the gel consistently. The mixing technique that we used was to take one 10 mL Luer lock syringe with alginate, another with cross-linker and mix the two back-and-forth through a Luer lock stopcock. We found a successful mixing procedure to be 10 full-cycle pumps at a rate of 1 pump per second. In consideration of resolution and shearing constraints, a 0.030” diameter syringe tip was chosen.

GEL PRINTING EXPERIMENTS

Unseeded Gel Printing Test

This experiment verified the ability of this system to print gels of complex arbitrary geometries. In this experiment, various geometries were printed on the gantry robot in full-scale, non-sterile printing runs. The following “proof of concept test pieces” were chosen because they each demonstrate the unique capabilities of this technology and because they have interesting medical applications.



Figure 8 - Test Piece 1: Meniscus-Shaped Single Material Gel (Above Are the CAD

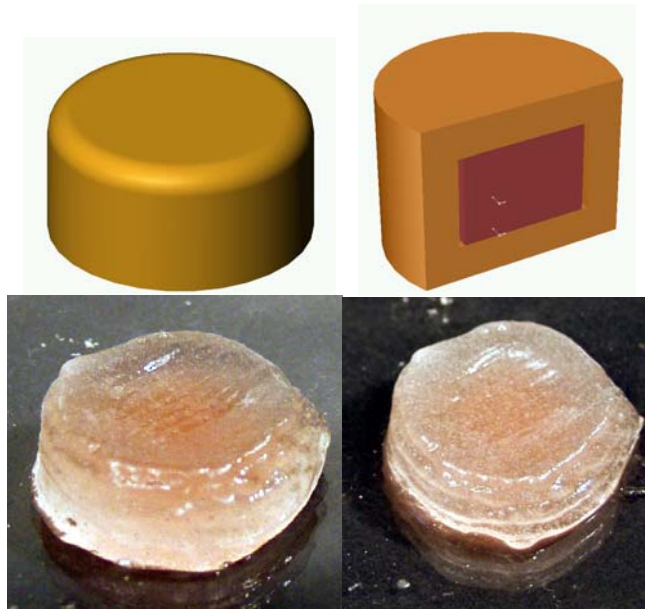


Figure 9 - Test Piece 2: Two Gel Embedded Piece (Red Dyed Gel Embedded in Clear

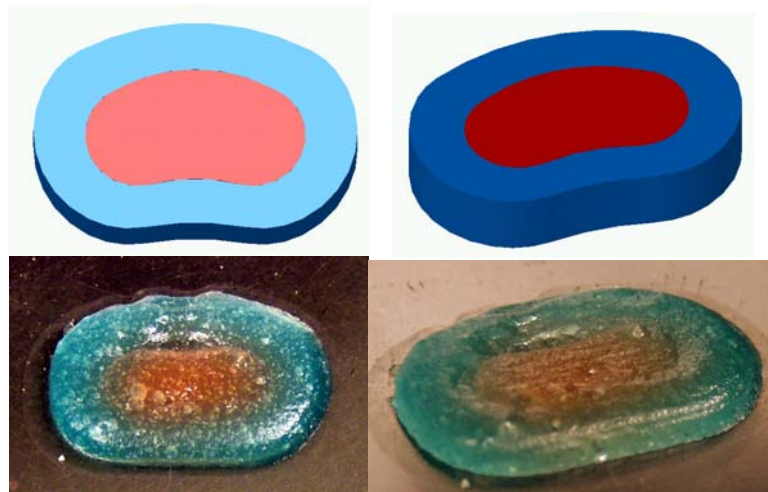


Figure 10 - Test Piece 3: Intervertebral Disk-Shaped, Two Material, Spatially

Viability of Seeded/Printed Gel Test

The viability test verified short-term cellular survivability. In other words, the test determined whether the gel sustained life throughout the printing process, i.e., while being subjected to the shear forces induced by the deposition process.

During viability testing, the printing process was simulated and then the percentage of living cells versus dead cells was measured before and after the simulated printing process (Fig. 11). In order to count the percentage of living cells, two fluorescent chemical markers were used. Calcein acetoxymethyl (calcein AM) attaches to living cells and ethidium homodimer-1 (EthD-1) attaches to dead cells. Through the use of a fluorescent light source, a microscope, and the

appropriate optical filters, the living and dead cells were identified (figs. 13, 14). The viability test did not have to be done under sterile conditions; the test was measuring short-term viability and infection would only have a long-term effect.



Figure 11 - Isometric View of Deposition Tool and Printer Before Printing Into a Petri Dish

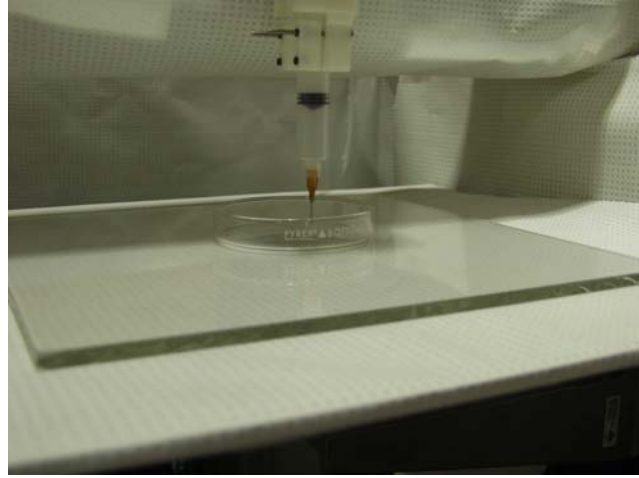


Figure 12 - Side View of Deposition Tool During Experiment

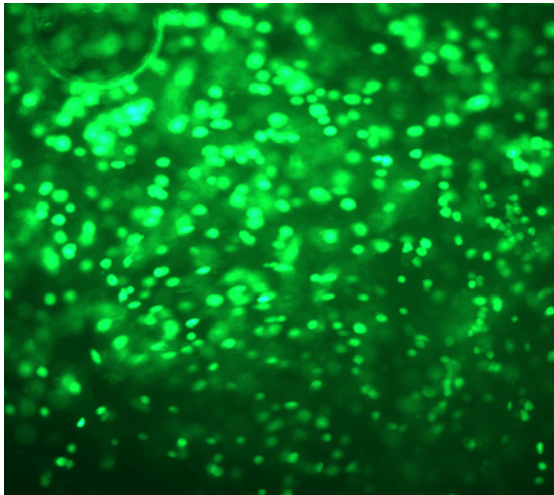


Figure 13 – Microscope View During Viability Test using Fluorescence Microscopy (Filtered to illuminate living cells)

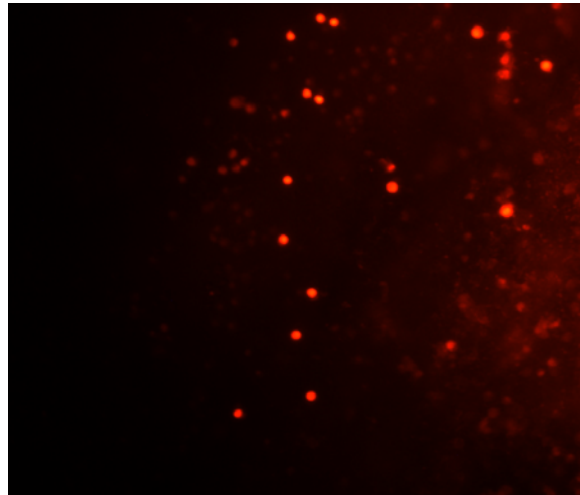


Figure 14 – Microscope View During Viability Test using Fluorescence Microscopy (Filtered to illuminate dead cells)

Process Sterility Test

The approach of using an autoclavable plastic bag as a printing envelope had to be tested to verify that no bacteria or fungi were allowed to infect the printed alginate gel. A sterile sample of alginate gel was prepared and placed in a sterile syringe. This syringe was then transported, with a sterilized syringe end-cap, to the printer and the full printing procedure was executed. After the printing, the sample was brought back to a sterile work hood where the envelope was opened and the sample removed. The gel sample was incubated for a period of eight days. After this incubation period, the sample was analyzed for presence of bacteria and fungi growth with

the use of a chemical marker and fluorescence microscopy. It was determined that there was less than 1 bacterium per 0.9 μL after 8 days of incubation; hence, the bag envelope concept was proven to be a success.

Direct CT Scan Printing Test

This research additionally demonstrated the ability to efficiently print a hydrogel implant directly from a CT Scan. A CT Scan of a meniscus cartilage was provided by the Cornell affiliated Hospital for Special Surgery (HSS) and then converted into an STL file. The STL file was then loaded into the CCSL software package and prepared for printing. The results of this direct CT Scan print are shown below.

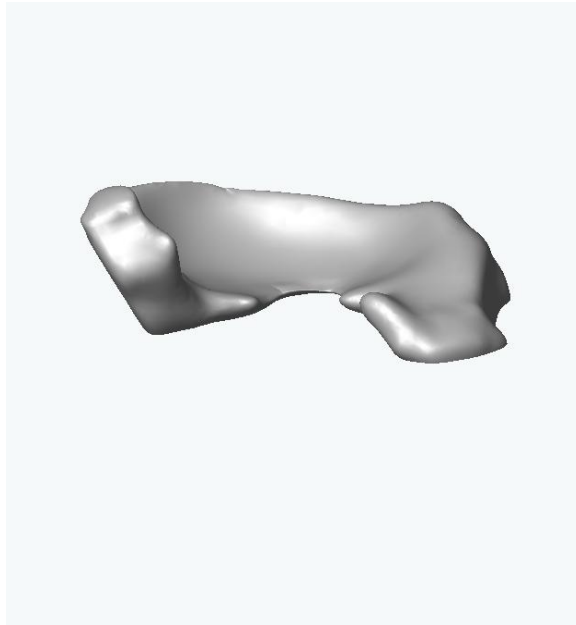
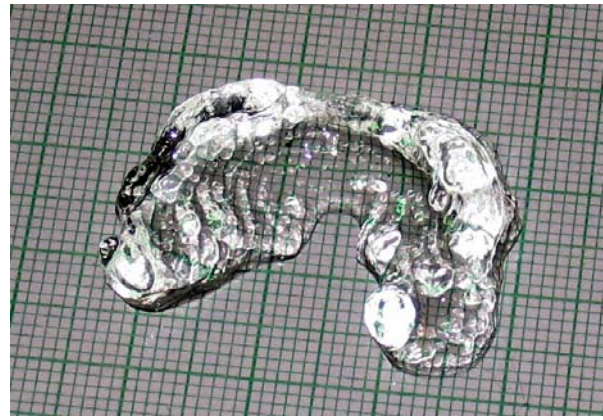


Figure 15 - Meniscus-Shaped Piece from CT Scan During Printing (above) and CAD Model Used for Print (below)

Figure 16 - Mensicus-Shaped Piece After Printing (above) and CAD Model Used for Print (below)

CONCLUSIONS

We have demonstrated the ability to successfully 3-D print viable, infection-free, living hydrogel implants of multiple materials. By printing with pre-cell-seeded alginate hydrogels, this technology serves as a versatile tissue engineering platform on which spatially heterogeneous implants of varied seeding densities, chemical concentrations, cell-types, etc. can be fabricated in arbitrary geometries. Additionally, the fabrication of implants generated directly from CT Scans brings this technology one step closer to its clinical form. This will allow patients to, within hours, have a complex, living, pre-seeded, multi-cell-type implant, such as an intervertebral disk, produced from prior CT Scans of their own healthy body parts.

BIBLIOGRAPHY

1. *Alginate Structure and Behavior*. London South Bank University.
<<http://www.lsbu.ac.uk/water/hyalg.html>>.
2. Chang S.C., Tobias G., Roy A.K., Vacanti C.A., Bonassar L.J., "Tissue engineering of autologous cartilage for craniofacial reconstruction by injection molding", *Plastic Reconstructive Surgery, Plast. Reconstr. Surg.* 112:3, 2003.
3. Evan Malone, Kian Rasa, Daniel Cohen, Todd Isaacson, Hilary Lashley, Hod Lipson, (2004) "Freeform fabrication of 3D zinc-air batteries and functional electro-mechanical assemblies", *Rapid Prototyping Journal*, Vol. 10, No. 1, pp. 58-69.
4. E. Sachlos and J.T. Czernuszka, (2003) "Making Tissue Engineering Scaffolds Work", *European Cells and Materials Journal*, Vol. 5, pp. 29-40.
5. Vladimir Mironov, Thomas Boland, Thomas Trusk, Gabor Forgacs, Roger Markwald, (2003) "Organ printing: Computer-aided jet-based 3D tissue engineering", *Trends in Biotechnology*, Vol. 21, No. 4, pp. 157-61.
6. Xu J.W., Zaporozhan V., Peretti G.M., Roses R.E., Morse K.B., Roy A.K., Mesa J.M., Randolph M.A., Bonassar L.J., Yaremchuk M.J., "Injectable tissue-engineered cartilage with different chondrocyte sources", *Plast. Reconstr. Surg.* 113:5, 2004.